Supplemental information: Intracellular coupling modulates biflagellar synchrony

Hanliang Guo[1,2], Yi Man[1], Kirsty Wan[3*], Eva Kanso[1*]

[1] Aerospace & Mechanical Engineering, University of Southern California, Los Angeles, CA 90089, USA
[2] Mathematics, University of Michigan, Ann Arbor, MI 48109, USA
[3] Living Systems Institute, University of Exeter, Exeter, EX4 4QD, UK

1 Filament model and numerical implementation

The balance of forces and moments on a cross section of the filament are given by Kirchhoff's equations for an elastic rod [1],

$$\mathbf{N}' - \mathbf{f} = \mathbf{0}, \qquad \mathbf{M}' + \hat{\mathbf{t}} \times \mathbf{N} = \mathbf{0}. \tag{1}$$

Here, the prime $(\cdot)' = (\cdot)_s = \partial(\cdot)/\partial s$ denotes differentiation with respect to arc-length s, $\hat{\mathbf{t}} = \mathbf{r}'/|\mathbf{r}'|$ is the tangent unit vector along the filament centerline. A schematic depiction of the model is shown in Figure 1.

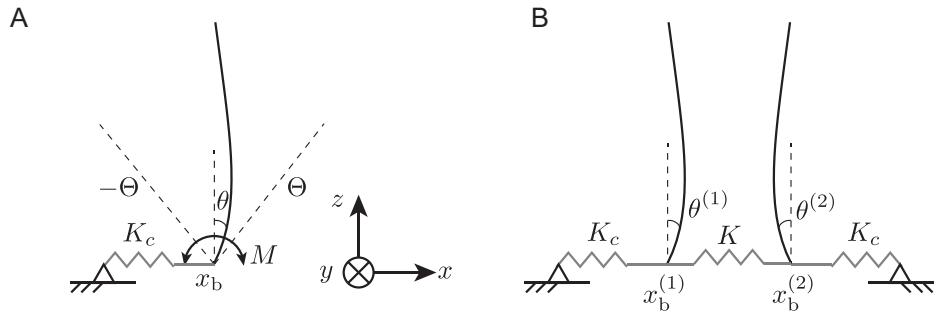

Figure 1: Filament model. A: Single filament connected to the base by a linear spring with stiffness K_c. The base is constrained to move along the x direction. B: Two filaments connected by a linear spring with stiffness K between the bases.

Integrate the force equation in (1) from the filament free end at ℓ to any location $s > 0$ along the filament, taking into account that $\mathbf{N}(\ell) = 0$, we have $\mathbf{N}(s) = \int_\ell^s \mathbf{f} \mathrm{d}s$. Similarly, integrating the moment equation in (1) yields, after an integration by parts on the second term,

$$\mathbf{M}(s) + \mathbf{r}(s) \times \int_\ell^s \mathbf{f}(\tilde{s}) \mathrm{d}\tilde{s} - \int_\ell^s \mathbf{r}(\tilde{s}) \times \mathbf{f}(\tilde{s}) \mathrm{d}\tilde{s} = \mathbf{0}. \tag{2}$$

The base of the filament is attached to a linear spring of stiffness K_c that is free to move in the horizontal plane. From the force balance of the entire filament in the x-direction, we arrive at

*Corresponding authors: K.y.wan2@exeter.ac.uk, Kanso@usc.edu

a boundary condition at the filament base

$$-K_{\rm c}\,x_{\rm b}-\mathbf{e}_x\cdot\int_0^{\ell}\mathbf{f}\mathrm{d}s=0, \tag{3}$$

where $x_{\rm b}(t)$ is the instantaneous position of the filament base; the basal point is constrained to move in the horizontal plane only yielding another boundary condition $\mathbf{r}(0,t)\cdot\mathbf{e}_z=0$, which is more conveniently enforced as a velocity constraint

$$\mathbf{r}_t(0,t)\cdot\mathbf{e}_z=0, \tag{4}$$

with proper initial configuration.

We discretize the filament into a uniform chain of $N+1$ beads separated by distance $\Delta s=\ell/N=a$. The beads are labeled from $n=0$ at the filament base to $n=N$ at its tip. The position vector is discretized by $\mathbf{r}_n=x_n\mathbf{e}_1+z_n\mathbf{e}_3$ and the local orientation θ_n of the tangent vector to bead n is defined as the angle between the z-axis and the vector $\Delta\mathbf{r}_n=(\mathbf{r}_{n+1}-\mathbf{r}_n)$. Let $\mathbf{F}_m$ be the force exerted by the m-th bead on the fluid, equation (2) can be written in discrete form as follows

$$\mathbf{M}_{n-1}+\mathbf{r}_{n-1}\times\left(-\sum_{m\geq n}^{N}\mathbf{F}_m\right)-\left(-\sum_{m\geq n}^{N}\mathbf{r}_m\times\mathbf{F}_m\right)=0\Rightarrow\mathbf{M}_{n-1}+\sum_{m\geq n}^{N}[(\mathbf{r}_m-\mathbf{r}_{n-1})\times\mathbf{F}_m]=\mathbf{0}. \tag{5}$$

Here, $\mathbf{M}_n=B\left[(\theta_n-\theta_{n-1})/\Delta s\right]\mathbf{e}_2$ is the elastic bending moment for $1\leq n<N$, whereas $\mathbf{M}_o=\pm M\mathbf{e}_2$ is the active driving moment at the base $z=0$. Let s_m be the arclength of the m-th bead, we note that $\mathbf{F}_m\approx\int_{s_m-\epsilon/2}^{s_m+\epsilon/2}\mathbf{f}(s,t)\mathrm{d}s=\int_{(m-\frac{1}{2})\Delta s}^{(m+\frac{1}{2})\Delta s}\mathbf{f}\mathrm{d}s$ is the discrete version of the volume force density $\mathbf{F}(\mathbf{x})=\int_0^{\ell}\mathbf{f}(s,t)\delta(\mathbf{x}-\mathbf{r}^{(\mathrm{i})}(s,t))\mathrm{d}s$.

Following the derivations in [2], the force exerted by bead $n\geq 1$ on the surrounding fluid can be written as $\mathbf{F}_n=\mathbf{F}_n^{\perp}+\mathbf{F}_n^{\parallel}$, where

$$\mathbf{F}_n^{\perp}=\left[-\mathbf{M}_{n-1}-\sum_{m>n}^{N}(\mathbf{r}_m-\mathbf{r}_{n-1})\times\mathbf{F}_m\right]\times\frac{\Delta\mathbf{r}_{n-1}}{\|\Delta\mathbf{r}_{n-1}\|^2}, \tag{6}$$

and for $1\leq n<N$

$$\mathbf{F}_n^{\parallel}=-K_e\left[-\frac{\|\Delta\mathbf{r}_n\|-\Delta s}{\Delta s}\frac{\Delta\mathbf{r}_n}{\|\Delta\mathbf{r}_n\|}\cdot\frac{\Delta\mathbf{r}_{n-1}}{\|\Delta\mathbf{r}_{n-1}\|}+\frac{\|\Delta\mathbf{r}_{n-1}\|-\Delta s}{\Delta s}\right]\frac{\Delta\mathbf{r}_{n-1}}{\|\Delta\mathbf{r}_{n-1}\|}, \tag{7}$$

whereas for $n=N$, one has

$$\mathbf{F}_N^{\parallel}=-K\frac{(\|\Delta\mathbf{r}_{N-1}\|-\Delta s)}{\Delta s}\frac{\Delta\mathbf{r}_{N-1}}{\|\Delta\mathbf{r}_{N-1}\|}. \tag{8}$$

Using (6) and (7-8), $\mathbf{F}_n$ can be evaluated sequentially from the filament tip (by decreasing order of n) to the second last segment ($n=1$) in terms of the filament kinematic variables $\mathbf{r}_m$, $m\geq n-1$.

The force at the base in the x direction $\mathbf{F}_o\cdot\mathbf{e}_x$ could be directly obtained from a discrete form of equation (3):

$$\mathbf{F}_o\cdot\mathbf{e}_x=-K_c(\mathbf{r}_o\cdot\mathbf{e}_x)-\sum_{n=1}^{N}\mathbf{F}_n\cdot\mathbf{e}_x, \tag{9}$$

whereas the force at base in the z direction $\mathbf{F}_o\cdot\mathbf{e}_z$ is found using (4) together with the hydrodynamic forces as detailed below.

Parameter	Symbol	Dimensionless value
Number of segments per filament	N	20
Segment length	$\Delta s = a$	5×10^{-2}
Total integration time	T	20
Basal switch angle	Θ	0.05π – 0.45π
Basal driving moment	M	1 – 3
Basal inter-filamentous spring stiffness	K	10 – 100
Basal filament-cell spring stiffness	K_c	10

Table 1: Dimensionless parameters used in simulations (ℓ, μ and B are normalized to 1).

To account for the fluid drag forces, we use a one-dimensional distribution of regularized Stokeslets along the centerline of the filament [3]. The regularized Stokeslets are placed at the center $\mathbf{r}_n$ of each segment. The strength of the regularized Stokeslet at $\mathbf{r}_n$ is equal to the discrete force $\mathbf{F}_n$ and the fluid velocity generated by the filament at an arbitrary position $\mathbf{x}$ in the fluid domain is given by

$$\mathbf{u}(\mathbf{x}) = \sum_{n=0}^{N} \mathbf{G}(\mathbf{x} - \mathbf{r}_n) \cdot \mathbf{F}_n, \tag{10}$$

where $\mathbf{G}(\mathbf{x}-\mathbf{r}_n)$ is the Green's tensor for the regularized Stokeslet [3]. We write the fluid boundary conditions

$$\mathbf{u}(\mathbf{x}, t)|_{\text{centerline}} = \mathbf{r}_t(s, t), \quad \mathbf{r}_t(0, t) \cdot \mathbf{e}_z = 0. \tag{11}$$

Recall (6) and (7-8) to express $\mathbf{F}_{n>0}$ in terms of the filament position $\mathbf{r}_m$, while $\mathbf{F}_o$ could be expressed in terms of $\mathbf{G}$ and $\mathbf{F}_{n>0}$ using (9), (10) and (11). This yields a set of coupled equations for the filament dynamics that we evolve forward in time using the time integrators for stiff equations with adaptive time step and prescribed error tolerances (MATLAB's ode15s). Initial conditions for this system are the configuration of the filament $\mathbf{r}(s, t)$ and the direction of the basal moment.

In all numerical simulations, we use $N = 20$ segments of length $a = 1/20$ to discretize the filament, and we set the regularization parameter of the Stokeslet to be equal to a. The tensile stiffness $K = 500$ is a numerical parameter chosen to keep the length of the filament almost constant (no more than 1% change in length). The filaments are initialized in straight configuration normal to the z plane. Here, we choose the relative and absolute error tolerance to be 10^{-6} and 10^{-10} respectively. The system is integrated to at least $T = 20$, which is sufficient to capture the long-time dynamics. See Table 1 for a summary of all parameter values.

2 Chlamydomonas-inspired beating

In the flagellum model (Figure 1C in the main text and Figure 2), the bending moment is set to $M = 2.5$ during the power stroke and $M = 1.25$ during the recovery stroke. The basal stiffness parameters are set to $K = 15$ and $K_c = 10$. The basal switch angles are $\Theta = 0.2\pi$ for freestyle and $\Theta = 0.1\pi$ for freestyle. Additionally, the basal switch angles are shifted 'outwards' by $\bar{\Theta} = 0.25\pi$ following *in vivo* observations. The bending stiffness linearly decays from the base to the tip $B(s) = 1 - s$. The reference curvature depends on the stroke- and arc-length as follows

$$\kappa_o(s) = \begin{cases} 0, & 1/4 < s < 3/4 \\ 1.5\pi, & \text{else} \end{cases} \tag{12}$$

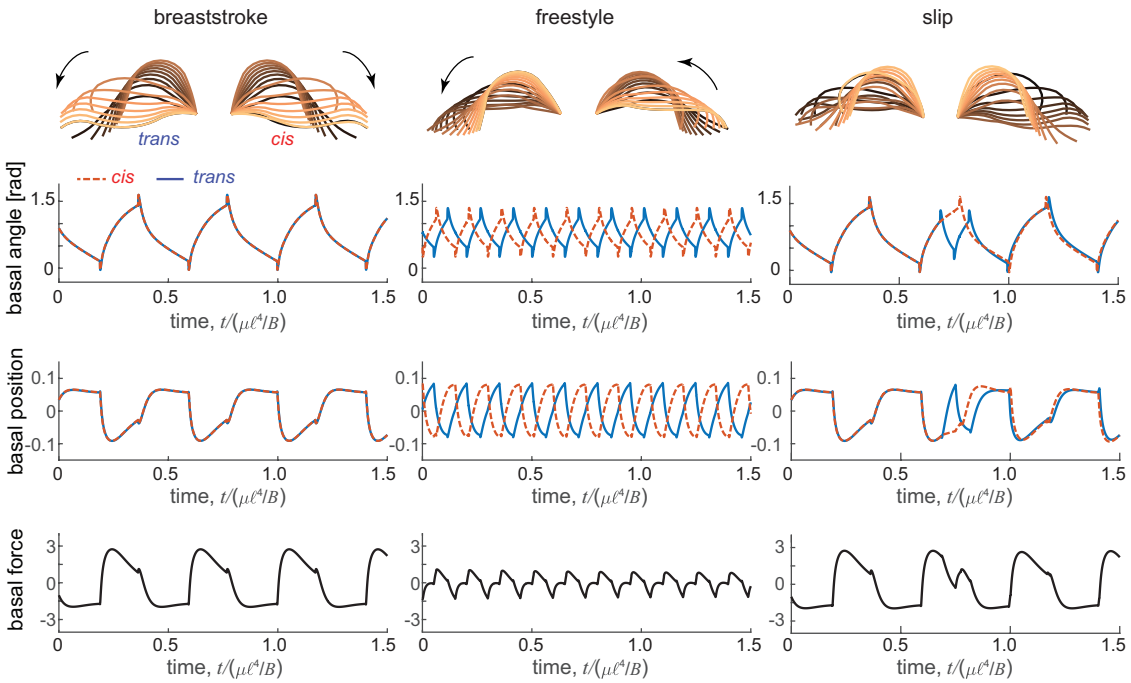

Figure 2: Filament pair model: snapshots of the *Chlamydomonas*-inspired beating waveforms during one beating period and time evolutions of basal angles, basal positions, and basal spring force showing inphase ($\Theta = 0.2\pi$), antiphase ($\Theta = 0.1\pi$), and phase-slip. The bases of the flagella are fixed in the snapshots for aesthetic purposes. Following the convention of the basal angles, the positive directions of the basal positions are taken to be 'outward'.

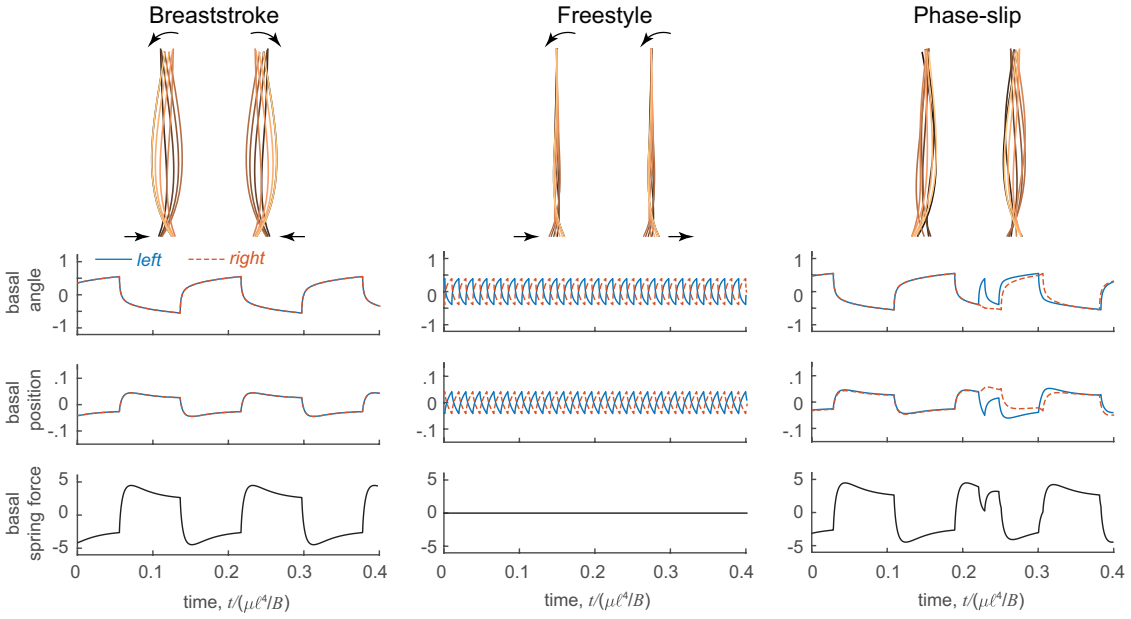

Figure 3: Filament pair model: snapshots of symmetric actuation beating waveforms and time evolutions of basal angles, basal positions, and basal spring force showing inphase ($\Theta = 0.175\pi$), antiphase ($\Theta = 0.125\pi$), and phase-slip. $K = 50$, $K_c = 10$, $M = 2$.

during power stroke, and

$$\kappa_o(s) = \begin{cases} 1.5\pi, & 1/4 < s < 3/4 \\ 0, & \text{else} \end{cases} \tag{13}$$

during recovery stroke.

Figure 2 shows snapshots of the filaments and the time evolution of the basal angles, basal positions, and basal spring force for the *Chlamydomonas*-inspired beating accompanying Figure 1C in the main text.

Figure 3 shows snapshots of the filaments and the time evolution of the basal angles, basal positions, and basal spring force for the symmetrically-actuated filaments accompanying Figure 2 in the main text.

3 Dumbbell model

Consider a dumbbell with two beads of radius a connected by a inextensible rod of length ℓ. The lower bead is hooked to the origin by a linear spring of stiffness K_c and is constrained to move in the $\mathbf{e}_x$ direction. Let x_b be the position of the lower bead along the $\mathbf{e}_x$-direction and $\mathbf{x} = x_\mathrm{b}\mathbf{e}_x + \ell\sin\theta\mathbf{e}_x + \ell\cos\theta\mathbf{e}_y$ be the position of the upper bead, with θ being the angle between the $\mathbf{e}_y$ axis and the dumbbell; see Figure 4A.

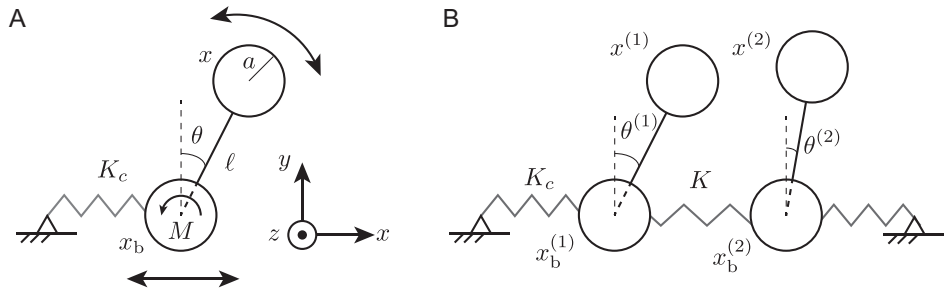

Figure 4: Dumbbell model. A: Single dumbbell connected to the base by a linear spring with stiffness K_c. The lower bead is constrained to move along the x direction. B: Two dumbbells connected by a linear spring with stiffness K between the bases.

The balance of force and moments on the dumbbell lead to two scalar equations governing the motion of $x_\mathrm{b}(t)$ and $\theta(t)$,

$$K_c x_\mathrm{b} + \xi(\dot{x}_\mathrm{b} + \ell\dot{\theta}\cos\theta) + \xi\dot{x}_\mathrm{b} = 0, \qquad \xi\ell(\cos\theta\dot{x}_\mathrm{b} + \dot{\theta}\ell) + M = 0 \tag{14}$$

where the drag coefficient $\xi = 6\pi\mu a$ is given by Stokes' law, and M is the driving moment.

In the case of two dumbbells, one gets the system of equations for the basal position $\dot{x}_\mathrm{b}^{(1)}, \dot{x}_\mathrm{b}^{(2)}$ and orientation angles $\dot{\theta}^{(1)}, \dot{\theta}^{(2)}$ of the two dumbbells

$$\begin{bmatrix} 2 & \ell\cos\theta^{(1)} & 0 & 0 \\ \cos\theta^{(1)} & \ell & 0 & 0 \\ 0 & 0 & 2 & \ell\cos\theta^{(2)} \\ 0 & 0 & \cos\theta^{(2)} & \ell \end{bmatrix} \begin{pmatrix} \dot{x}_\mathrm{b}^{(1)} \\ \dot{\theta}^{(1)} \\ \dot{x}_\mathrm{b}^{(2)} \\ \dot{\theta}^{(2)} \end{pmatrix} = -\frac{1}{\xi} \begin{pmatrix} K_c x_\mathrm{b}^{(1)} + K\left(x_\mathrm{b}^{(1)} - x_\mathrm{b}^{(2)}\right) \\ M^{(1)}/\ell \\ K_c x_\mathrm{b}^{(2)} + K\left(x_\mathrm{b}^{(2)} - x_\mathrm{b}^{(1)}\right) \\ M^{(2)}/\ell \end{pmatrix}. \tag{15}$$

Note that the off-diagonal submatrices are identically zero because we do not consider hydrodynamic coupling between the two dumbbells. The basal coupling terms appear in the right-hand-side only.

To non-dimensionalize the system, we pick ℓ as the characteristic length scale, ℓK_c as the force scale, and ξ/K_c as the time scale. The dimensional variables in the equations can be written in

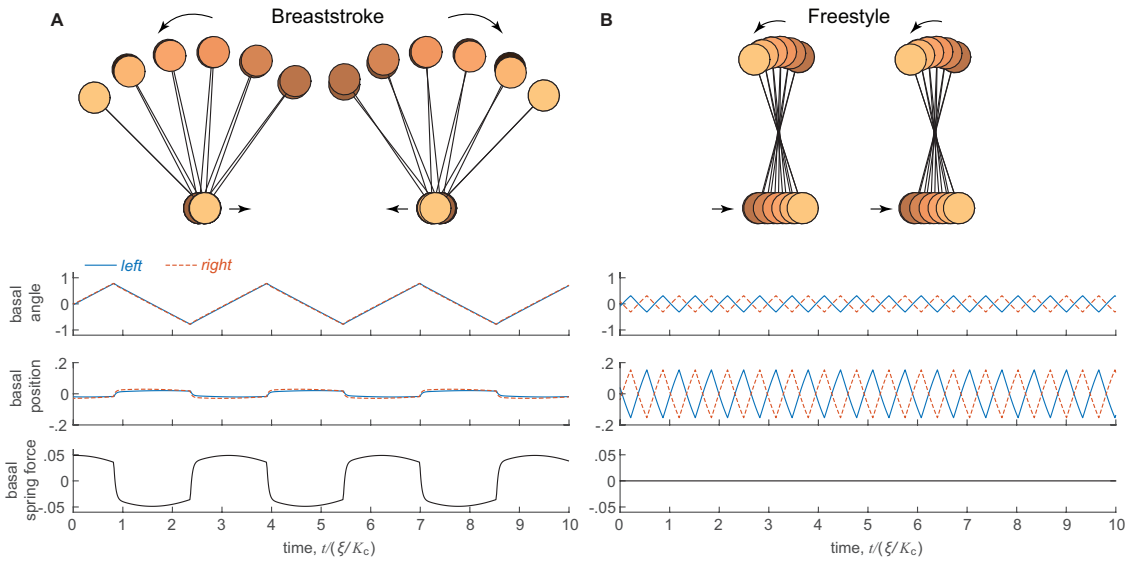

Figure 5: Dumbbell pair model: snapshots of dumbbell configuration and time evolutions of basal angles, basal positions, and basal spring force for (A) breaststroke ($\Theta = 0.25\pi$) and (B) freestyle ($\Theta = 0.1\pi$) synchrony. Parameter values are set to $K = 20$, $M = 1$.

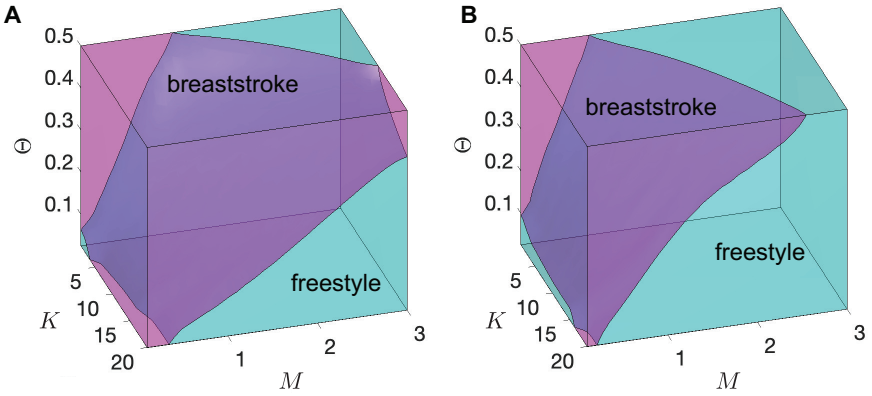

Figure 6: Long-term dynamics of the dumbbell model over the full 3D parameter space. A: long-term dynamics of the dumbbell model with breaststroke initial condition; B: long-term dynamics of the dumbbell model with freestyle initial condition.

terms of combinations of scales and dimensionless variables: $x_\mathrm{b} = \ell\tilde{x}_\mathrm{b}$, $t = (\xi/K_\mathrm{c})\tilde{t}$, $M = \ell^2 K_\mathrm{c}\tilde{M}$, $K = K_c\tilde{K}$. Consequently, the dimensionless counterparts of (15) is

$$\begin{bmatrix} 2 & \cos\theta^{(1)} & 0 & 0 \\ \cos\theta^{(1)} & 1 & 0 & 0 \\ 0 & 0 & 2 & \cos\theta^{(2)} \\ 0 & 0 & \cos\theta^{(2)} & 1 \end{bmatrix} \begin{pmatrix} \dot{\tilde{x}}_\mathrm{b}^{(1)} \\ \dot{\tilde{\theta}}^{(1)} \\ \dot{\tilde{x}}_\mathrm{b}^{(2)} \\ \dot{\tilde{\theta}}^{(2)} \end{pmatrix} = - \begin{pmatrix} \tilde{x}_\mathrm{b}^{(1)} + \tilde{K}(\tilde{x}_\mathrm{b}^{(1)} - \tilde{x}_\mathrm{b}^{(2)}) \\ \tilde{M}^{(1)} \\ \tilde{x}_\mathrm{b}^{(2)} + \tilde{K}(\tilde{x}_\mathrm{b}^{(2)} - \tilde{x}_\mathrm{b}^{(1)}) \\ \tilde{M}^{(2)} \end{pmatrix}, \tag{16}$$

where $\tilde{}$ denotes the dimensionless variables. Figure 5 shows snapshots of the coupled dumbbell and the time evolution of basal angles, basal positions, and basal spring force accompanying Figure 5 of the main text.

The long-term dynamics of basally connected dumbbells with two initial conditions are shown

in Figure 6. Data points in magenta color are the dumbbells synchronized into breaststroke synchrony, while data points in cyan color are the dumbbells synchronized into freestyle synchrony. The different long-term dynamics between the two initial conditions is the result of the bistability.

4 Mechanism driving synchrony extended to stiff filaments

The mechanism driving synchrony (β) could be extended to stiff filaments ($B \to \infty$). Specifically, the relaxation time for the rigid filament would be $T_\mathrm{b} = \xi_\perp \ell / K$, where $\xi_\perp$ is the drag coefficient for the filament in the direction perpendicular to its centerline. The intrinsic oscillation time T_a could be obtained by moment balance $M = \xi_\perp \dot{\theta} \int_0^\ell s^2 \mathrm{d}s = \xi_\perp (\Theta / T_\mathrm{a}) \ell^3 / 3 \Rightarrow T_\mathrm{a} = \frac{\xi_\perp \ell^3 \Theta}{3M}$. The ratio between T_b and T_a is thus $\beta = \dfrac{3M}{K\ell^2\Theta}$, which is different from that of the minimal model by only a constant factor 3. For finite filament compliance B, we expect a nonlinear relationship between $M/K\ell^2$ and Θ.

References

[1] Basile Audoly and Yves Pomeau. *Elasticity and geometry: from hair curls to the non-linear response of shells*. Oxford University Press, 2010.

[2] Hanliang Guo, Lisa Fauci, Michael Shelley, and Eva Kanso. Bistability in the synchronization of actuatedmicrofilaments. *Journal of Fluid Mechanics*, 836:304?323, 2018.

[3] Ricardo Cortez and Douglas Varela. A general system of images for regularized stokeslets and other elements near a plane wall. *Journal of Computational Physics*, 285:41–54, 2015.